Am J Cancer Res 2019;9(5):999-1008
www.ajcr.us /ISSN:2156-6976/ajcr0092823

Original Article

Aberrant shuttling of long noncoding RNAs during the mitochondria-nuclear crosstalk in hepatocellular carcinoma cells

Yijing Zhao[1,2], Shanshan Liu[1,2], Lei Zhou[1,2], Xueli Li[1,2], Ying Meng[1,2], Yan Li[1,2], Lingyu Li[1], Benzheng Jiao[1,2], Ling Bai[1], Yu Yu[1], Songling Zhang[1], Wei Li[1], Andrew R Hoffman[2], Ji-Fan Hu[1,2], Jiuwei Cui[1]

[1]*Key Laboratory of Organ Regeneration and Transplantation of Ministry of Education, Cancer Center, The First Hospital of Jilin University, Changchun 130021, Jilin, China;* [2]*Stanford University Medical School, VA Palo Alto Health Care System, Palo Alto, CA 94304, USA*

Received February 20, 2019; Accepted April 4, 2019; Epub May 1, 2019; Published May 15, 2019

Abstract: There is intense crosstalk between mitochondria and the nucleus that is mediated by proteins and long noncoding RNAs (lncRNAs). Using a modified RNA fluorescent *in situ* hybridization (RNA-FISH) assay coupled with MitoTracker staining, we tracked the mitochondrial localization of lncRNAs, including lncND6 and lncCytB. The nuclear genome-transcribed lncRNA MALAT1 was enriched in the mitochondria of hepatocellular carcinoma cells. Knockdown of MALAT1 significantly impaired mitochondrial function and alter tumor phenotype in HepG2 cells. The localization of the mitochondria-encoded lncRNA lncCytB was also abnormal in HepG2 cells. In normal hepatic HL7702 cells, lncCytB was located in mitochondria, but in HepG2 cells, it was enriched considerably in the nucleus. These data suggest that aberrant shuttling of lncRNAs, whether nuclear genome-encoded or mitochondrial genome-transcribed, may play a critical role in abnormal mitochondrial metabolism in cancer cells. This data lays the foundation for further clarifying the roles of mitochondria-associated lncRNAs in cancers.

Keywords: Mitochondria, lncRNAs, hepatocarcinoma, mitochondria-nuclear crosstalk, mitochondrial metabolism

Introduction

Mitochondria are essential cellular organelles that regulate energy generation, calcium signaling, and intrinsic apoptotic pathways in cancer [1, 2]. There exists a mitochondria-nuclear crosstalk that serves as a pathway of communication to influence many cellular and organismal activities. This bidirectional crosstalk can regulate several oncogenic pathways involved in tumorigenesis [3]. The mechanism whereby proteins are imported into mitochondria has been a topic of intense investigation [4, 5] ever since the first report of tRNA transport from cytoplasm to mitochondria a half-century ago [6].

The use of next-generation RNA sequencing has led to the surprising discovery that numerous nuclear genome-encoded long noncoding RNAs (lncRNAs), including RMRP and RPPH1, may localize to mitochondria [6-9]. Recent studies suggest that mitochondrial lncRNAs, whether encoded by the mitochondrial genome or encoded by the nuclear genome and then transported into the mitochondria, may play an essential role in mitochondrial metabolism [9-11]. In order to explore the physiologic roles of these lncRNAs, it would be ideal to have a method to actually visualize these molecules within an organelle in an individual cell. This would require a new approach, like RNA-fluorescent in situ hybridization (FISH), in conjunction with a method to simultaneously identify mitochondria.

In this paper, we used a modified RNA-FISH approach to track lncRNAs that are enriched within the mitochondria. Using this approach, we demonstrate the localization of both the mitochondria-encoded RNAs and nuclear genome-encoded lncRNAs in isolated mitochondria and in whole cells. We show that there was abnormal mitochondria-nuclear crosstalk

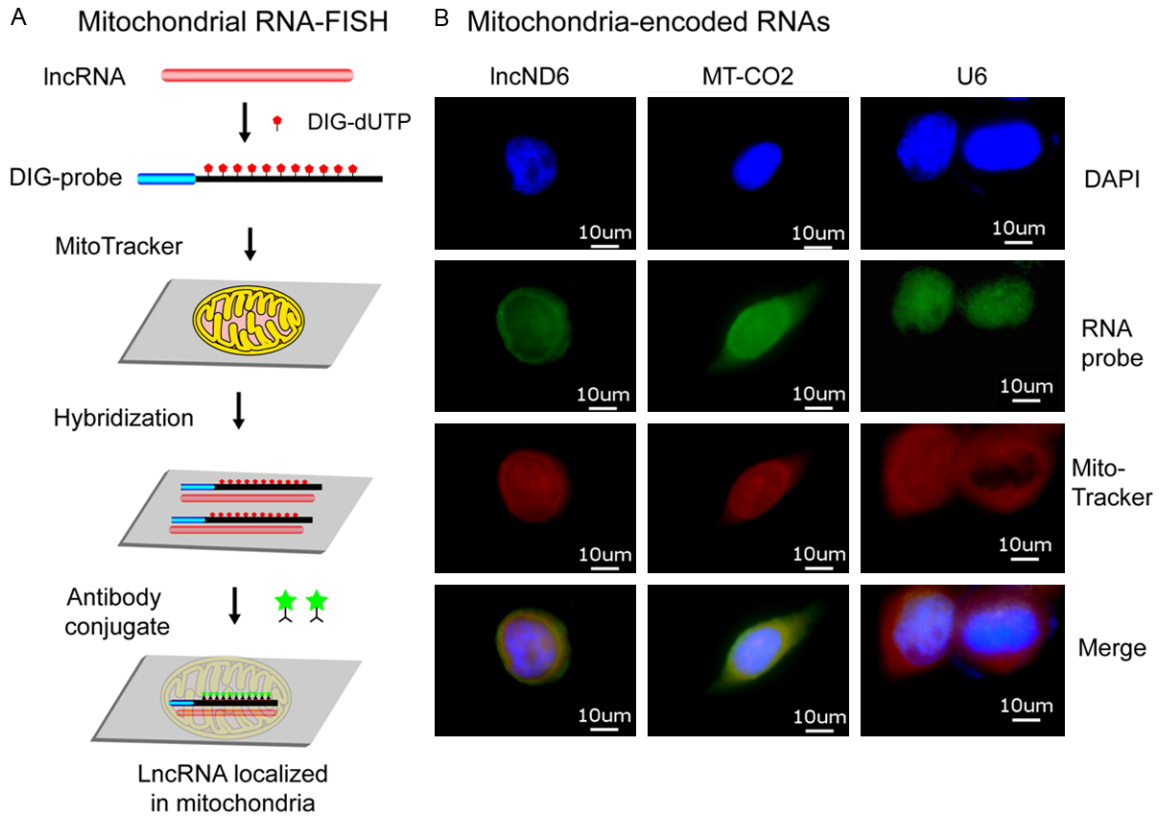

Figure 1. Detection of RNAs in mitochondria by the combined RNA fluorescent *in situ* hybridization (RNA-FISH) and MitoTracker staining. A. The principle of asymmetric PCR-derived single-stranded DNA probes in RNA-FISH for lncRNA localization in mitochondria. B. Mitochondrial localization of lncRNA lncND6. Mitochondria-encoded MT-CO2 RNA, as a mitochondrion positive control, is localized in mitochondria. U6 snRNA, encoded by the nuclear genome, is used as a negative control and is localized in the nucleus. MitoTracker was used to stain mitochondria. As expected, lncND6 is primarily located in the mitochondria of HepG2 cells.

of lncCytB in hepatoma cells, suggesting a new function of this lncRNA as a mitochondria-nuclear communicator in cancer cell homeostasis. We further show that the nuclear genome-encoded lncRNA MALAT1 was enriched in mitochondria, where it functions as a critical epigenetic player in the regulation of mitochondrial function. Together, this study greatly expands our knowledge of how nucleus-encoded lncRNAs can modulate the function of mitochondria.

Materials and methods

Hepatic cell lines

Hepatocellular carcinoma cell line HepG2 was purchased from ATCC and cultured in high glucose DMEM (Invitrogen, CA) supplemented with 10% FBS, 100 U/ml Penicillin-Streptomycin. Normal hepatic cell line HL7702 was purchased from the Type Culture Collection of the Chinese Academy of Sciences (Shanghai, China) and was cultured in high glucose DMEM supplemented with 20% FBS (Invitrogen, CA), 1× Non-Essential Amino Acid (NEAA, Invitrogen, CA) 100 U/ml Penicillin-Streptomycin (Invitrogen, CA). Cells were incubated at 37°C in 5% CO_2 air atmosphere.

Cell level RNA-FISH

We used a modified RNA-FISH assay to track lncRNAs in mitochondria (**Figure 1A**). In this assay, we used asymmetric PCR to selectively amplify the probe strand by adding digoxigenin-labeled dNTP. Asymmetric PCR was used to over-amplify the antisense strand of the cDNA template using an unbalanced ratio of primers. In asymmetric PCR, excessive amounts of the complementary primer were added to the reaction mixture. The method also required additional PCR cycles due to the slower amplification that occurred later in the reaction cycle,

when the limiting primer has been depleted [12]. By replacing dTTP with digoxigenin (DIG)-dUTP, asymmetric PCR synthesizes single-stranded, DIG-labeled DNA probes. In order to assess mitochondrial localization of lncRNAs, we counterstained the mitochondria by MitoTracker™ (MitoTracker™ Red CMXRos Cat: M7512 Invitrogen™) and lncRNAs using spectrally distinct fluorophores to verify their co-localization. The next step was to use FITC conjunct antibody to detect the lncRNA interacted probe. This increased the output signal by using secondary reporters that bind to the hybridization probes.

Mitochondrial level RNA-FISH

Mitochondria are not the only organelles in the cytoplasm. To rule out the possibility that lncRNAs are located within the cytoplasm but outside of the mitochondria, we performed the RNA-FISH staining method in isolated mitochondria. Mitochondria isolation was performed following the protocol provided by the Mitochondria isolation kit (Qproteome Mitochondria Isolation Kit. Cat: 37612). Before mitochondria isolation, live mitochondria were stained by MitoTracker™. After mitochondria isolation, RNA-FISH was applied to the mitochondria slides. The detailed reagents and step-by-step procedure are summarized in Supplementary Materials and the primers for asymmetric PCR are listed in Table S1.

MALAT1 knockdown

To study the role of MALAT1 in HepG2 cells, we used shRNAs to knockdown MALAT1. Briefly, short hairpin RNAs (shRNAs) against the 3' region of MALAT1 mRNA were inserted into a lentiviral vector. The shMALAT1 1# sequence was 5'-CACAGGGAAAGCGAGTGGTTGGTAA-3' and shMALAT1 2# sequence was 5'-GATCCATAATCGGTTTCAAGGTA-3'. After confirmation by DNA sequencing, the lentiviruses were packaged in 293T cells using polyethylenimine (PEI, 5 μg/μl). The virus-containing supernatants were collected and concentrated with centrifugal Filter Units (Amicon Ultra-15, Millipore, MA). HepG2 cells in 6-well plates were infected with lentiviruses using polybrene (8 μg/ml). Three days after infection, HepG2 cells were selected by puromycin, and mixed stable cells were collected for each shRNA group and used for gene analysis by RT-PCR.

ATP determination assay

The ATP levels in control HepG2 and shMALAT1 cells were measured by an Enhanced ATP Assay Kit (S0027, Beyotime Biotechnology, Shanghai, China), according to the manufacturer's instructions [13]. The concentration of ATP was calculated according to an ATP standard curve and expressed as nmol/OD730. ATP levels were reported as nmol/mg of protein.

Transwell assay

Cell migration capability was measured using a 6-well Corning BioCoat Matrigel Invasion Chamber with a membrane. About 5×10^4 cells in 2.0 ml high glucose DMEM media without FBS were placed into the upper chambers. The lower chambers were filled with 2.5 ml complete medium with 10% FBS as a chemo-attractant stimulus. After incubation for 24 hours at 37°C, non-invading cells were removed from the top of the chamber with a cotton swab. Migrated cells on the bottom surface of the filter were fixed, stained with 0.5% crystal violet, and counted in five random fields under a microscope, and the average number of five fields was calculated.

Epithelial-mesenchymal transition (EMT) model establishment

TGF-β has been shown to be a key driver of hepatocellular oncogenesis, promoting EMT [14]. Therefore, we used TGF-β1 as an EMT inducer. EMT was induced by TGF-β1 (PeproTech, Rocky Hill, NJ) following the reported protocol [15, 16]. Briefly, cells were seeded into 15cm plates. Following 24 h incubation, EMT-inducing medium (containing 10ng/ml TGF-β1) was used to replace the common medium and the cells were incubated for an additional 72 h.

Cellular fractionation assay

As previously described [17], cellular fractions were separated by NE-PER Nuclear and Cytoplasmic Extraction Reagents (Thermo Scientific) with RNase inhibitor (Thermo Scientific). After separation, RNAs were extracted from nuclear and cytoplasmic fractions using Trizol (Life Technologies, Carlsbad, CA), and were converted into cDNA with the SuperScript™ III RT (Invitrogen). The real-time Q-PCR was performed using 2X RealStar Power SYBR Mixture

(GenStar A311). The relative expression was calculated on the basis of CT values against an internal standard curve for each specific set of primers. The data were normalized over the value of β-actin control.

Results

Localization of mitochondrial DNA-encoded lncRNAs by RNA-FISH

To study the role of lncRNAs in mitochondria-nuclear crosstalk, we used a modified RNA-FISH method to detect the localization of mitochondria-associated long non-coding RNA and protein-coding RNA in mitochondria (**Figure 1A**). The mitochondria-encoded MT-CO2 mRNA was chosen as a positive control. As expected, MT-CO2 mRNA was located in the mitochondria, as seen by the green fluorescence of the RNA that merged with the red-stained mitochondria using MitoTracker (**Figure 1B**, orange). U6, a well-known nuclear lncRNA, was chosen as a negative control [18]. As expected, the U6 probe overlapped with DAPI staining in the nucleus (**Figure 1B**, cyan). We also observed that lncND6, a mitochondria-encoded lncRNA [19], was localized in mitochondria.

Nuclear genome-encoded lncRNAs (NG-lncRNAs) in mitochondria

To study the shuttling of lncRNAs between the mitochondria and the nucleus, we also performed the RNA-FISH assay for nuclear genome-encoded lncRNAs, including RMRP (RNA component of mitochondrial RNA processing endoribonuclease) and RPPH1 (ribonuclease P RNA component H1). The mitochondrial localization of these two lncRNAs was previously discovered by mitochondria RNA-sequencing [6, 7], but had not been confirmed by RNA-FISH. Mitochondria are not the only cytoplasmic organelles, so to rule out the possibility that lncRNAs are located in the cytoplasm but outside of the mitochondria, we applied this staining method to isolated mitochondria.

Figure 2A showed that RMRP and RPPH1 were located in the isolated mitochondria. Compared with whole cell FISH, this method avoids interference from other cytoplasmic organelles. The abundance of the lncRNAs varied from one mitochondrion to another. When there was a high abundance of lncRNAs in the mitochondria, the FISH color was yellow. When lncRNAs are not abundant, the color appeared to be more orange. Both lncRNAs were abundantly localized in mitochondria.

We also compared the location of these two lncRNAs in whole cells. The nucleus was stained with the DAPI dye. As shown in **Figure 2B**, the lncRNA probe (green) overlaid with MitoTracker™ (red) and the merged color changed from red to orange, depending on the abundance of the lncRNAs. Thus, our modified mitochondrial RNA-FISH method can be used to track the exchange of lncRNAs between the nucleus and mitochondria.

Aberrant shuttling of lncRNA lncCytB in hepatoma cells

We also compared the mitochondria-nuclear localization of mitochondrial DNA-encoded lncRNAs between hepatoma and normal hepatic cells. LncCytB is a mitochondria-encoded lncRNA. In normal liver HL7702 cells, RNA-FISH staining indicated that lncCytB was localized primarily in the mitochondria. In hepatoma HepG2 cells, however, we found that lncCytB was not only present in the mitochondria but was also detected in the nucleus (**Figure 3A**). Notably, the abundance of lncCytB was much higher in the nucleus.

We also used the cellular fractionation assay to confirm the location of lncCytB in the nucleus in HepG2 cells. Cytoplasmic and nuclear RNAs were isolated and were reverse transcribed into cDNAs. Using Q-PCR, we also confirmed that the abundance of lncCytB was significantly higher in the nucleus than in the cytosol (**Figure 3B**).

Accumulating evidence supports the role of epithelial-mesenchymal transition (EMT) in tumor cell progression, invasion, and metastasis. Such transformation promotes cancer migration and invasion. We thus examined if EMT would alter the localization of lncRNAs. We induced EMT in HepG2 cells using TGF-β1 and performed RNA-FISH to check the localization of lncCytB. We fund that EMT did not significantly alter the localization of lncCytB in the nucleus (**Figure 3C**).

Collectively, these data suggest that lncCytB may function as a messenger communicating between the nucleus and mitochondria. Further

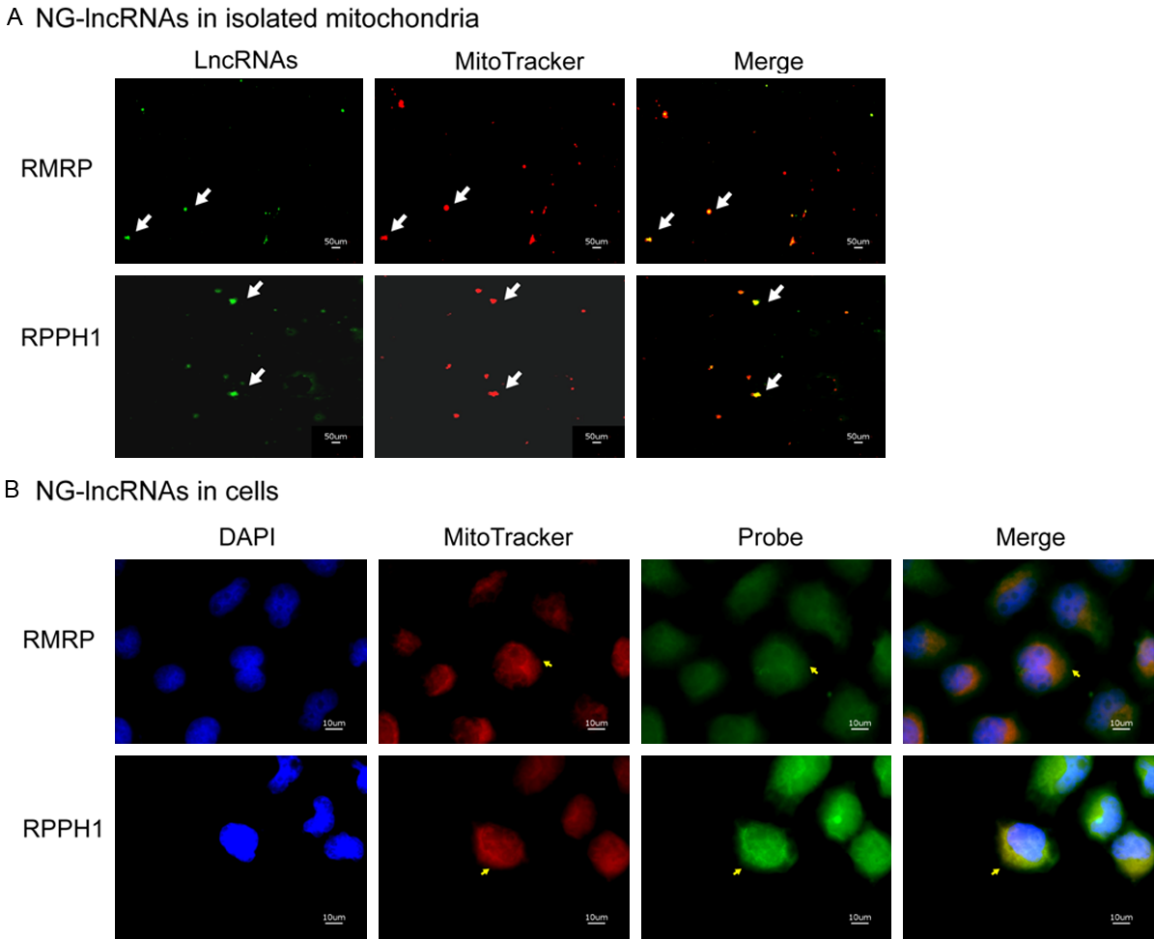

Figure 2. Detection of the nuclear-encoded lncRNAs in mitochondria. A. Detection of the nuclear-encoded lncRNAs in mitochondria on isolated mitochondria smear slides. MitoTracker was used to stain mitochondria (red). RMRP and RPPH1 are shown in isolated mitochondria (arrows). B. Staining of the nuclear-encoded lncRNA RMRP and RPPH1 in the mitochondria of HepG2 cells. DAPI was used to stain nuclear DNA. MitoTracker was used to stain mitochondria. Arrows: the merged color of lncRNAs (green) and MitoTracker (red).

studies are needed to address whether the aberrant location of the lncCytB may relate to characteristic malignant characteristics of the cancer cell, such as the Warburg effect [20].

The role of nuclear genome-encoded MALAT1 in mitochondria

Currently, we know very little about the role of the mitochondria-localized lncRNAs, particularly those that are encoded in the nuclear genome. Metastasis-associated lung adenocarcinoma transcript 1 (MALAT1) was originally thought to be a nucleus-enriched lncRNA [21]. Recently, we found that the nuclear genome-encoded MALAT1 was also enriched in mitochondria in hepatoma HepG2 cells. Thus, we isolated mitochondria and performed RNA-FISH on smear slides. We found that the probe enriched area (green) coincided with that of the MitoTracker staining (**Figure 4A**). Thus, MALAT1, although encoded by the nuclear genome, was also enriched in the mitochondria collected from HepG2 cells.

We then used PCR to compare the abundance of MALAT1 in the mitochondria from normal hepatic HL7702 cells and from hepatoma HepG2 cells (**Figure 4B**). As the positive controls, the mitochondrial genome-encoded ND5 and ND6 mRNAs were detected in both cells (lanes 3-4). However, we found that MALAT1 was abundantly enriched in the HepG2 mitochondria, but was barely detectable in the HL7702 mitochondria (lane 2). Further studies are needed to compare mitochondrial MALAT1 in clinical samples, including hepatoma, the adjacent tissues, and normal hepatic tissues.

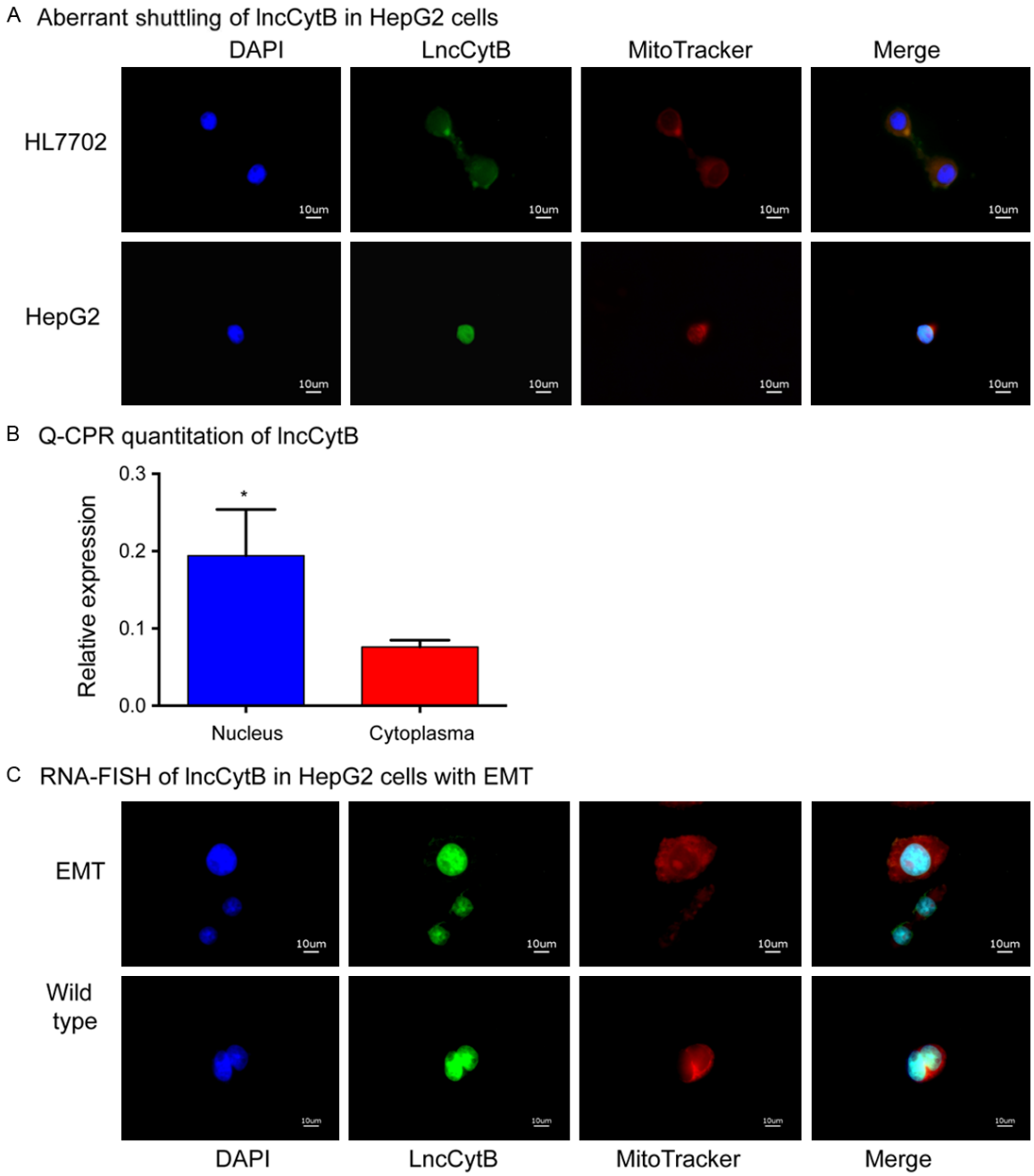

Figure 3. Differential positioning of the mitochondrial-encoded lncRNA lncCytB in normal liver cells (HL7702), hepatoma cells (HepG2) and HepG2-EMT. A. RNA-FISH staining. In HL7702 cells, lncCytB is primarily located in mitochondria. In HepG2 cells, however, lncCytB is aberrantly transported to the nucleus. B. Q-PCR quantitation. The cellular fractionation assay showed lncCytB is largely enriched in the nucleus compared to the cytoplasm. *P = 0.0277, unpaired *t*-test. C. RNA-FISH in HepG2-wild type and HepG2-EMT cells. After induction of EMT with TGF-β1, cells were stained by RNA-FISH. The mitochondrial genome-encoded lncRNA lncCytB is dominated in the nucleus.

To understand the role of MALAT1 in mitochondrial biogenesis and energetics, we knocked down MALAT1 using shRNA lentiviruses in hepatoma HepG2 cells. We found that the MALAT1-deficient HepG2 cells produced less ATP than the vector and random shRNA control cells (**Figure 4C**). Therefore, the mitochondrial enrichment of MALAT1 may be a critical process to regulate energy metabolism in HepG2 cells.

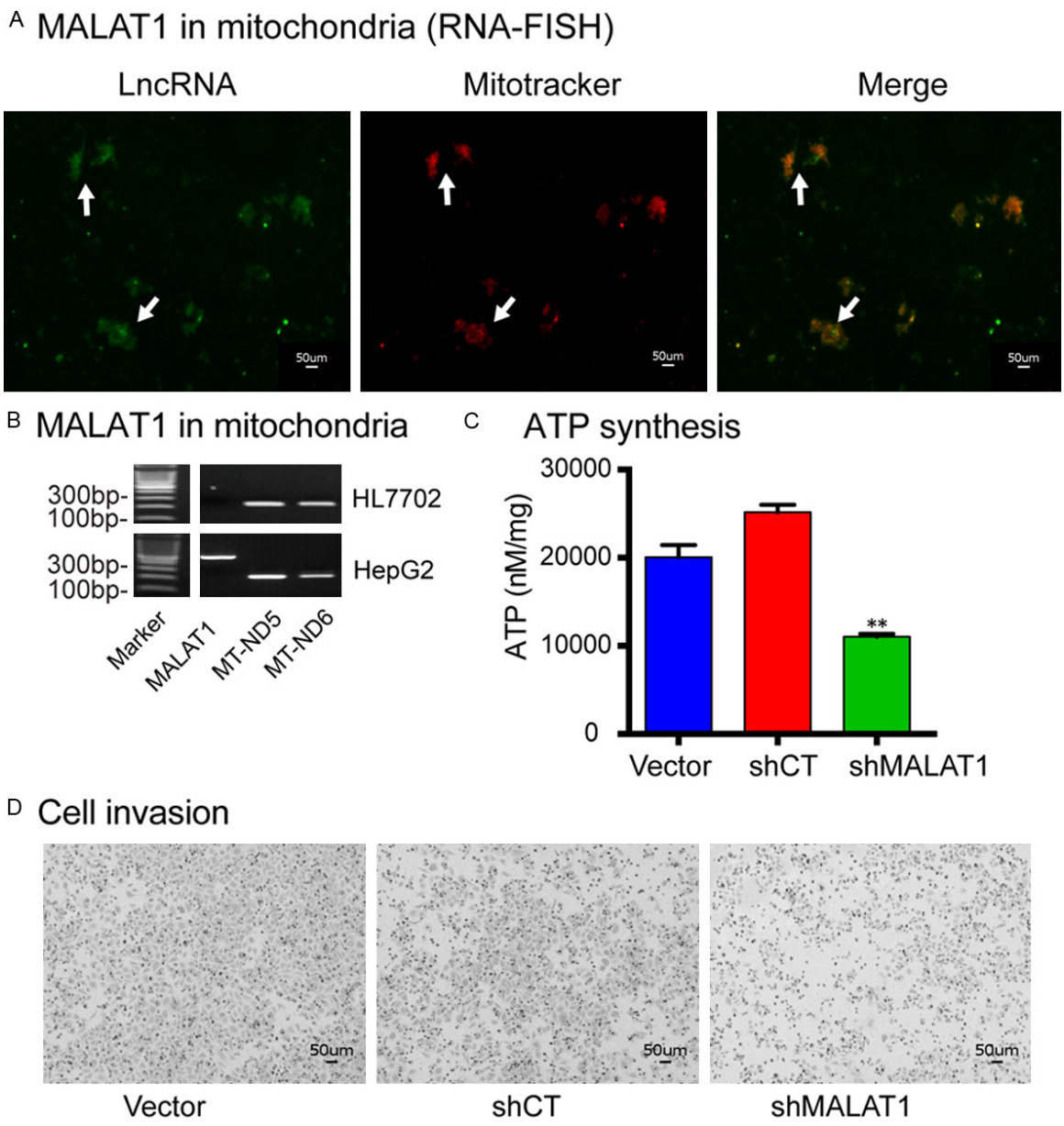

Figure 4. The nuclear lncRNA MALAT1 is enriched in HepG2 mitochondria. A. RNA-FISH of MALAT1 in isolated HepG2 mitochondria. MALAT1 is localized in the isolated mitochondria that are stained in red with the MitoTracker dye. B. Differential enrichment of MALAT1 lncRNA in the mitochondria of normal and malignant cells. HepG2: hepatocellular carcinoma cell; HL7702: normal hepatic cell; MT-ND5 and MT-ND6: mitochondrial ND5 and ND6 mRNAs as the positive control. Note that MALAT1 is barely detectable in normal H7702 mitochondria. C. MALAT1 knockdown impaired the mitochondrial ATP production ability. ** $P < 0.01$, ordinary one-way ANOVA. D. Knockdown of MALAT1 significantly inhibited invasion of HepG2 cell.

We examined if knockdown of MALAT1 will affect the tumor phenotype in HepG2 cells. Using the Transwell assay, we showed that cell invasion was lower in shMALAT1-treated cells than that in vector control (Vector) and shRNA random control (shCT) cells (**Figure 4D**). These results indicate that down-regulation of MALAT1 impaired the cell invasion *in vitro*.

Discussion

An intense crosstalk between mitochondria and the nucleus, mediated by proteins as well as ncRNAs, is required for cellular homeostasis [22]. Using a modified RNA-FISH, we tracked the mitochondrial localization of the lncRNAs lncND6 and lncCytB in hepatocellular carcino-

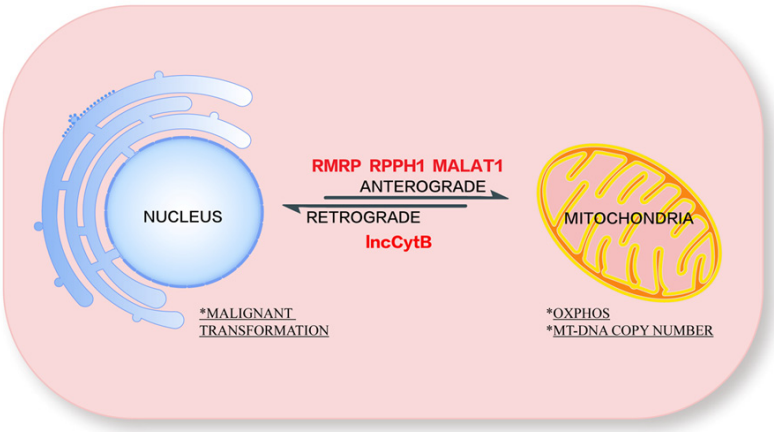

Figure 5. The model of the mitochondria-nuclear shuttling of lncRNAs. RMRP, RPPH1, and MALAT1 are all the nuclear genome-encoded lncRNAs. They function as anterograde signals to communicate between the mitochondria and the nucleus. On the other hand, lncCytB is a mitochondrial genome-encoded retrograde signal. It shuttles from the mitochondria to the nucleus in hepatoma cells. The aberrant shuttling of lncRNAs in this mitochondria-nucleus crosstalk may be associated with abnormal energy metabolism in malignant cells.

ma cells (HepG2) and normal hepatic cells (HL7702). Interestingly, we demonstrated that the oncogenic lncRNA MALAT1 that is encoded by the nuclear genome, is also enriched in the HepG2 mitochondria. Using shRNA knockdown, we show that MALAT1 is critical for maintaining normal mitochondrial function. The mitochondria-encoded lncRNA lncCytB, on the other hand, is aberrantly transported to the nucleus in hepatoma HepG2 cells as compared with normal hepatic HL7702 cells. Collectively, our data reveal a previously unreported shuttling of lncRNAs during the mitochondria-nucleus crosstalk. The aberrant shuttling of lncRNAs in this crosstalk may be associated with abnormal energy metabolism in hepatoma cells (**Figure 5**).

RMRP is the first reported lncRNA that is encoded by a single-copy gene in the nucleus and then imported into mitochondria [23]. Using *in situ* hybridization analysis, Li and colleagues showed that RMRP is present in mitochondria, though with a relatively low abundance as compared with the nucleus [24]. In this study, using HepG2 cells as a model we also showed the presence of considerable amounts of RMRP in mitochondria, confirming that nuclear lncRNAs can shuttle from the nucleus to mitochondria.

MALAT1, a nuclear genome-encoded lncRNA, has previously been associated with tumorigenicity in a variety of malignancies [25, 26]. It regulates the expression of metastasis-associated genes and cell motility at the transcriptional and/or post-transcriptional levels, regulating the activity of motility-related genes [27, 28]. Since MALAT1 regulates mitochondrial apoptosis and mitophagy, it has been suggested that MALAT1 may function as a regulator of mitochondrial metabolism [22, 29, 30]. Our study provides evidence that MALAT1 may act as a nucleus-to-mitochondria messenger, as MALAT1 is transported from the nucleus to the mitochondria in hepatoma HepG2 cells. Knockdown of MALAT1 affects mitochondrial function. These data suggest that after being transported into mitochondria, MALAT1 may directly alter mitochondrial metabolism in hepatoma cells. In normal hepatic HL7702 cells, however, the level of MALAT1 in mitochondria is very low. It will be interesting to explore if mitochondrial MALAT1 is associated with disease progression and tumor survival.

Our results support the concept that retrograde and anterograde signaling occurs as lncRNAs shuttle between the nucleus and mitochondria crosstalk [8, 9]. In this crosstalk (**Figure 5**), lncRNAs function as epigenetic messengers, altering mitochondrial metabolism during oncogenesis. In this study, we show that the mitochondrial genome-encoded lncCytB is a typical example of a signaling lncRNA. In normal liver HL7702 cells, lncCytB is localized primarily in the mitochondria. In hepatoma HepG2 cells, however, this lncRNA is transported into the nucleus. Future work is needed to determine the mechanism underlying this translocation or shuttling.

In summary, this study greatly expands our knowledge that the nucleus-encoded lncRNAs, like MALAT1, may act as epigenetic regulators to alter the mitochondrial function. The mitochondria-derived lncRNAs, on the other

hand, may also shuttle into the nucleus, where they may regulate target genes related to tumor phenotypes. This study thus suggests novel biological functions for lncRNAs and lays the foundation for further clarifying the roles of mitochondrial lncRNAs.

Acknowledgements

This work was supported by the National Key R&D Program of China (2018YFA0106902), the Key Project of Chinese Ministry of Education grant (311015), the National Basic Research Program of China (973 Program) (2015CB943303), Nation Key Research and Development Program of China grant (2016YFC13038000), National Natural Science Foundation of China (31430021, 81874052, 81672275, 31871297, 81670143), Research on Chronic Noncommunicable Diseases Prevention and Control of National Ministry of Science and Technology (2016YFC1303804), National Health Development Planning Commission Major Disease Prevention and Control of Science and Technology Plan of Action, Cancer Prevention and Control (ZX-07-C2016004), Natural Science Foundation of Jilin Province (20150101176JC, 20180101117JC, 20130413010GH), and California Institute of Regenerative Medicine (CIRM) grant (RT2-01942); and the Department of Veterans Affairs (BX002905).

Disclosure of conflict of interest

None.

Address correspondence to: Dr. Jiuwei Cui, Cancer Center, The First Hospital of Jilin University, 71 Xinmin Street, Changchun 130021, China, Tel: +86 431-8878-2178; E-mail: cuijw@jlu.edu.cn; Dr. Ji-Fan Hu, Department of Medicine, PAVIR, VA Palo Alto Health Care System, Palo Alto, CA 94304, USA, Tel: 650-852-3175; Fax: 650-856-8024; E-mail: jifan@stanford.edu; Dr. Andrew R. Hoffman, Medical Service, Stanford University Medical School, 3801 Miranda Ave., Palo Alto, CA 94304, Tel: 650-858-3930; Fax: 650-856-8024; E-mail: arhoffman@stanford.edu

References

[1] Singh KK and Costello LC. Mitochondria and cancer. springer, 2009.

[2] Corbet C and Feron O. Cancer cell metabolism and mitochondria: nutrient plasticity for TCA cycle fueling. Biochimica et Biophysica Acta (BBA) - Reviews on Cancer 2017; 1868: 7-15.

[3] Mello T, Simeone I and Galli A. Mito-Nuclear Communication in Hepatocellular Carcinoma Metabolic Rewiring. Cells 2019; 8: E417

[4] Chacinska A, Koehler CM, Milenkovic D, Lithgow T and Pfanner N. Importing mitochondrial proteins: machineries and mechanisms. Cell 2009; 138: 628-644.

[5] Schmidt O, Pfanner N and Meisinger C. Mitochondrial protein import: from proteomics to functional mechanisms. Nat Rev Mol Cell Biol 2010; 11: 655-667.

[6] Kim KM, Noh JH, Abdelmohsen K and Gorospe M. Mitochondrial noncoding RNA transport. BMB Rep 2017; 50: 164-174.

[7] Noh JH, Kim KM, Abdelmohsen K, Yoon JH, Panda AC, Munk R, Kim J, Curtis J, Moad CA, Wohler CM, Indig FE, de Paula W, Dudekula DB, De S, Piao Y, Yang X, Martindale JL, de Cabo R and Gorospe M. HuR and GRSF1 modulate the nuclear export and mitochondrial localization of the lncRNA RMRP. Genes Dev 2016; 30: 1224-1239.

[8] Zhao Y, Sun L, Wang RR, Hu J-F and Cui J. The effects of Mitochondria-associated long noncoding RNAs in cancer mitochondria: new players in an old arena. Critical Reviews in Oncology/Hematology 2018;

[9] Dong Y, Yoshitomi T, Hu JF and Cui J. Long noncoding RNAs coordinate functions between mitochondria and the nucleus. Epigenetics Chromatin 2017; 10: 41.

[10] Vendramin R, Marine JC and Leucci E. Noncoding RNAs: the dark side of nuclear-mitochondrial communication. EMBO J 2017; 36: 1123-1133.

[11] Wang Y, Hu SB, Wang MR, Yao RW, Wu D, Yang L and Chen LL. Genome-wide screening of NEAT1 regulators reveals cross-regulation between paraspeckles and mitochondria. Nat Cell Biol 2018; 20: 1145-1158.

[12] Heiat M, Ranjbar R, Latifi AM, Rasaee MJ and Farnoosh G. Essential strategies to optimize asymmetric PCR conditions as a reliable method to generate large amount of ssDNA aptamers. Biotechnol Appl Biochem 2017; 64: 541-548.

[13] Zhou J, Zhang F, Meng H, Zhang Y and Li Y. Introducing extra NADPH consumption ability significantly increases the photosynthetic efficiency and biomass production of cyanobacteria. Metab Eng 2016; 38: 217-227.

[14] Giannelli G, Villa E and Lahn M. Transforming growth factor-beta as a therapeutic target in hepatocellular carcinoma. Cancer Res 2014; 74: 1890-1894.

[15] Moreno-Bueno G, Peinado H, Molina P, Olmeda D, Cubillo E, Santos V, Palacios J, Portillo F and Cano A. The morphological and molecular features of the epithelial-to-mesenchymal transition. Nat Protoc 2009; 4: 1591-1613.

[16] Xu Z, Shen MX, Ma DZ, Wang LY and Zha XL. TGF-beta1-promoted epithelial-to-mesenchymal transformation and cell adhesion contribute to TGF-beta1-enhanced cell migration in SMMC-7721 cells. Cell Res 2003; 13: 343-350.

[17] Li L, Li W, Chen N, Zhao H, Xu G, Zhao Y, Pan X, Zhang X, Zhou L and Yu D. FLI1 exonic circular RNAs as a novel oncogenic driver to promote tumor metastasis in small cell lung cancer. Clinical Cancer Research 2019; 25: 1302-1317.

[18] Spiller MP, Boon KL, Reijns MA and Beggs JD. The Lsm2-8 complex determines nuclear localization of the spliceosomal U6 snRNA. Nucleic Acids Res 2007; 35: 923-929.

[19] Rackham O, Shearwood AM, Mercer TR, Davies SM, Mattick JS and Filipovska A. Long noncoding RNAs are generated from the mitochondrial genome and regulated by nuclear-encoded proteins. RNA 2011; 17: 2085-2093.

[20] Liberti MV and Locasale JW. The Warburg Effect: How Does it Benefit Cancer Cells? Trends Biochem Sci 2016; 41: 211-218.

[21] Gutschner T, Hammerle M and Diederichs S. MALAT1 -- a paradigm for long noncoding RNA function in cancer. J Mol Med (Berl) 2013; 91: 791-801.

[22] De Paepe B, Lefever S and Mestdagh P. How long noncoding RNAs enforce their will on mitochondrial activity: regulation of mitochondrial respiration, reactive oxygen species production, apoptosis, and metabolic reprogramming in cancer. Curr Genet 2018; 64: 163-172.

[23] Topper JN, Bennett JL and Clayton DA. A role for RNAase MRP in mitochondrial RNA processing. Cell 1992; 70: 16-20.

[24] Li K, Smagula CS, Parsons WJ, Richardson JA, Gonzalez M, Hagler HK and Williams RS. Subcellular partitioning of MRP RNA assessed by ultrastructural and biochemical analysis. J Cell Biol 1994; 124: 871-882.

[25] Yu B and Shan G. Functions of long noncoding RNAs in the nucleus. Nucleus 2016; 7: 155-166.

[26] Wu Y, Huang C, Meng X and Li J. Long noncoding RNA MALAT1: insights into its biogenesis and implications in human disease. Current pharmaceutical design 2015; 21: 5017-5028.

[27] Tano K, Mizuno R, Okada T, Rakwal R, Shibato J, Masuo Y, Ijiri K and Akimitsu N. MALAT-1 enhances cell motility of lung adenocarcinoma cells by influencing the expression of motility-related genes. FEBS Lett 2010; 584: 4575-4580.

[28] Gutschner T, Hammerle M, Eissmann M, Hsu J, Kim Y, Hung G, Revenko A, Arun G, Stentrup M, Gross M, Zornig M, MacLeod AR, Spector DL and Diederichs S. The noncoding RNA MALAT1 is a critical regulator of the metastasis phenotype of lung cancer cells. Cancer Res 2013; 73: 1180-1189.

[29] Liang J, Liang L, Ouyang K, Li Z and Yi X. MALAT1 induces tongue cancer cells' EMT and inhibits apoptosis through Wnt/beta-catenin signaling pathway. J Oral Pathol Med 2017; 46: 98-105.

[30] Li LJ, Chai Y, Guo XJ, Chu SL and Zhang LS. The effects of the long non-coding RNA MALAT-1 regulated autophagy-related signaling pathway on chemotherapy resistance in diffuse large B-cell lymphoma. Biomed Pharmacother 2017; 89: 939-948.

Supplementary Materials

Detail RNA-FISH protocol

Reagents

a. Probe preparation
   1. 10 × Digoxigenin Labeling DNA Mix (Cat.11277065910, ROCHE): 1 mM dATP, 1 mM dCTP, 1 mM dGTP, 0.65 mM dTTP, 0.35 mM Digoxigenin-11-dUTP (DIG-dUTP), pH 7.5.
   2. Preparation of 3 × KlenTaq1 PCR reaction mixture: 10 × PC2 KlenTaq1 buffer 300 μl, Klentaq1 polymerase 7 μl (AB Bioscience, LLC), double-distilled water 543 μl.
   3. Mix Digoxigenin Labeling DNA Mix (1 mM) with KlenTaq PCR reaction buffer at a ratio of 3:17. Other PCR reaction kits may also work; the key is to exchange the normal dNTP mix with Digoxigenin Labeling DNA Mix.
b. Cell culture on coverslips
   1. Culture cells for at least 12 h on sterilized coverslips; if the cells are not adherent, gelatin-pretreated coverslips are recommended.
c. Mitochondria staining
   1. Mitotracker (MitoTracker™ Red CMXRos Cat: M7512 Invitrogen™). Note: MitoTracker™ regents come in many color choices. MitoTracker™ needs to be retained in the cells after fixation and permeabilization.
d. Fixation and permeabilization
   1. Fixation solution: freshly prepared and filter-sterilized 4% paraformaldehyde (PFA) in 1 × PBS.
   2. Fresh permeabilization solution: CSK buffer containing 0.2-0.5% v/v Triton X-100 (Sigma). Add an RNase inhibitor, 2 mM Vanadyl Ribonucleoside Complex (VRC) (Cat: S1042S, New England Biolabs), and 2 mM EGTA.
   3. CSK buffer: Cytoskeletal buffer (CSK): 10 mM PIPES, pH 7.0, 100 mM NaCl, 300 mM Sucrose, 3 mM $MgCl_2$. Filter, sterilize, and store in aliquots at -20°C.
e. RNA-FISH
   1. Anti-Digoxigenin-Fluorescein, Fab fragments (Cat: 11207741910, Roche).
   2. 20 × SSC buffer: 3 M sodium chloride, 0.3 M sodium citrate.
   3. Hybridization buffer: 10% Formamide, 2 × SSC prepared from, 10% w/v dextran sulfate (Cat. D8906, Sigma), 1 mg/mL Ecoli t-RNA (Cat. AM7119, Invitrogen™) and 2 mM VRC. Note: mix the dextran sulfate in water with gentle agitation at room temperature until dissolved, and then add other components. (500 μL aliquots and store at -20°C). Filter using 0.22 mm filters and store at -20°C in aliquots.
f. FISH on mitochondria smearing slides
   1. Mitochondria isolation kit (Qproteome Mitochondria Isolation Kit. Cat: 37612).

Detailed protocol

ssDNA probe preparation

For probe synthesis, the complementary strand of an lncRNA (targeting strand) is considered to be the "probe strand", which is amplified to excess using asymmetric PCR. The principle of asymmetric PCR-derived single-stranded DNA probes is shown in Figure S1A. To make a probe, the proper primer dilution ratio must be determined; the primer information is shown in Table S1.

In order to identify the optimal ratio of primers that produce the greatest amounts of ssDNA, serially dilute the targeting strand primer (forward primer) at ratios of 1:1, 1:10, 1:50, 1:100, and 1:500, with concentrations ranging from 0.01 to 5 μM. The concentration of reverse primer solutions in the experiment was fixed at 5 μM. Use a standard PCR reaction (PCR reaction system: 97°C, 2 min; 97°C, 30 s; 64°C, 30 s; 72°C, 30 s; 72°C, 10 min; for 38 cycles) with the dNTP mix containing Digoxigenin-dUTP. The PCR products are applied to a 2% agarose gel to check the results. The optimal primer ratio was selected as previously described [1].

Figure S1B shows the PCR product when the ratio of the two primer strands varied from 1:1 (lane 1) to 1:500 (lane 5). The band in lane 2 (1:10 ratio) is similar in intensity to that in lane 1, suggesting that the majority of products at this ratio are still double-stranded. In lanes 3, 4 and 5, the bands represent the asymmetric PCR products, which migrate on the gel differently from the double stranded DNA due to their secondary structure [1]. Therefore, we chose the dilution ratio (1:50) that produces the brightest single strand DNA bands on the gel, suggesting the greatest amplification efficiency for this asymmetric PCR reaction.

After choosing the optimal primer dilution ratio, the probe is then synthesized using the Digoxigenin-containing dNTP mix. The commonly used dNTP mix is replaced by Dig Labeling DNA Mix while the other components of the PCR reaction remain the same. To avoid the production of nonspecific bands, hot start PCR is recommended. The final product was assessed for size by electrophoresis on 2% agarose gels, in which each incorporated Dig-11-dUTP retards migration as if it were two specific bands. To precipitate the Dig-labeled DNA probe, two volumes of 100% ethanol, 10% 3 M sodium acetate (pH 5.2) and 1.5 μL of glycogen (20 mg/μl) are added. The samples were stored at -20°C for 30 minutes or overnight, and were centrifuged at full speed (> 10,000 × g) for 10 minutes. After centrifugation, supernatant is removed without disturbing the pellet. The pellet is rinsed three times with 400 μL of 70% ethanol. Using a pipette, the residual ethanol is aspirated without disturbing the pellet, and the pellet allowed to air dry (for about 5-10 minutes). The purified ssDNA is then suspended in 10 μl TE buffer. The DNA concentration is measured using the ssDNA detection model.

Mitochondria staining and cell fixation

HepG2 and HL7702 cell lines were cultured in DMEM with high glucose medium (HyClone, Logan, UT, USA) containing 10% fetal bovine serum, 20% fetal bovine serum, respectively (HyClone; GE Healthcare Life Sciences, Logan, UT, USA). The medium also contains 100 U/mL Penicillin-Streptomycin (ThermoFisher, Santa Clara, CA, USA), and the cells were incubated at 37°C with 5% CO_2. Cells are grown on slides (e.g. Superfrost Plus autoclaved glass slides - treated with 0.1% gelatin if the cells do not adhere- or plastic LabTek chamber slides from Nunc). Rinse slides in 1 × PBS at room temperature. In order to stain the mitochondria, cell samples are prepared following the MitoTracker™ kit instructions as described [2]. Add pre-warmed (37°C) staining solution containing the MitoTracker™ probe using working concentrations of 25-500 nM. The incubation time will vary depending on the model system and probe used. Incubate for 15-45 minutes under growth conditions. All of the following steps must be performed under very low light. For mitochondria RNA co-localization, it is important to note that fixing and permeabilizing the cells may cause the color to fade. Thus, a stable fluorophore in the MitoTracker™ kit is suggested. The cells are then fixed in 4% paraformaldehyde/1 × PBS for 10 min on ice. After permeabilizing the cells for 4-7 min (up to 15-30 minutes if needed) in fresh permeabilization solution, wash the slides twice in 70% ethanol, and store them in 70% ethanol at 4°C or -20°C for up to a month. Longer storage will lead to color fading.

Preparing the slide and hybridization

Dehydrate the slides in 80%, 95%, and 100% v/v ethanol for 3 min each and then air dry them on a 42°C heating plate. Resuspend the DNA probe in TE buffer at a final concentration of 4 ng/μL and vortex thoroughly to ensure complete resuspension of the labeled probe. Next, dilute the DNA probe in hybridization buffer to a final concentration of 1 ng/μL. If too much probe is added, a false positive signal may occur.

The DNA probe is then denatured by incubating it at 72°C for 5 minutes and then cooling the solution on ice. Apply 10 μL of the denatured DNA probe to one half of the specimen slide, cover with a 22 × 22 mm coverslip, and seal the edge of the coverslip with a bead of rubber cement. Incubate the slides at 37°C overnight. The following day, remove the coverslips carefully with forceps and wash the slides three times in 50% formamide, 2× SSC (adjusted to pH 7.2) for 5 min each at 42°C.

Fab fragments from an anti-digoxigenin antibody will be used in the next step, so slides must be incubated in a blocking buffer (PBS, 0.1% v/v Triton 100, 1% w/v BSA) for 30 min at room temperature in a humid chamber to reduce nonspecific signals. The slide is then incubated for 4 hours at room tempera-

ture with anti-digoxigenin-fluorescein diluted 1:50 to 1:500 (1:100 is the initial recommended solution) in blocking buffer.

For lncRNAs localized to the nucleus, DAPI counterstaining is achieved by incubating the cells in 20 ng/mL DAPI for five minutes at room temperature. Wash the slide three times for 5 min in PBS and allow it to air dry in the dark. Mount the coverslip and fix in place with a minimal amount of nail polish.

References

[1] Liang Z, Lao R, Wang J, Liu Y, Wang L, Huang Q, Song S, Li G and Fan C. Solubilization of single-walled carbon nanotubes with single-stranded DNA generated from asymmetric PCR. International Journal of Molecular Sciences 2007; 8: 705-713.

[2] Chazotte B. Labeling mitochondria with mitotracker dyes. Cold Spring Harb Protoc 2011; 2011: 990-992.

Table S1. Oligonucleotide primers

Gene	Primer name	Primer Sequence
RMRP	JH5636 RMRP-R1 (318 bp)	CTTCTGCAGGAATTCACAGCCGCGCTGAGAATGAGCC
	JH5637 RMRP-F1 (318 bp)	GGTTCGTGCTGAAGGCCTGTATCCT
RPPH1	JH5634 RPPH1-R1 (356 bp)	CTTCTGCAGGAATTCAATGGGCGGAGGAGAGTAGTCTGA
	JH5639 RPPH1-F1 (356 bp)	ATAGGGCGGAGGGAAGCTCATCAGT
MT-COX2	JH3291 hmtCox2-F1 (134 bp)	ATGGCACATGCAGCGCAAGTAGGTC
	JH3292 hmtCox2-R1 (134 bp)	GTTAGGAAAAGGGCATACAGGAC
lncND6	JH3185 lncND6-F1 (127 bp)	CAATGTTCAACCAGTAACTACTAC
	JH3186 lncND6-R1 (127 bp)	GGTAAACTTTAATAGTGTAGGAAGC
lncCYTB	JH3182 lncCyt-F1 (127 bp)	ATAGGGCAAGGACGCCTCCTAG
	JH3183 lncCyt-R1 (127 bp)	CCAGACAATTATACCCTAGCCA
MT-ND1	JH5809 mtND1-F1 (125 bp)	GCATACCCCCGATTCCGCTA
	JH5810 mtND1-R1 (125 bp)	TGAGGGGGAATGCTGGAGAT
MALAT1	JH5241 MALAT1-F (155 bp)	GTAATGCTGG GTGGGAACATG
	JH5242 MALAT1-R (155 bp)	CTAGCATCTTAGCGGA AGCTG
β-Actin	J880 β-actin-F (135 bp)	CAGGTCATCACCATTGGCAATGAGC
	J881 β-actin-R (135 bp)	CGGATGTCCACGTCACACTTCATGA
U6	SJ215 U6-F1 (103 bp)	GTGCTCGCTT CGGCAGCACA TATAC
	SJ216 U6-R1 (103 bp)	ATATGGAACGCTTCACGAATTTGCG

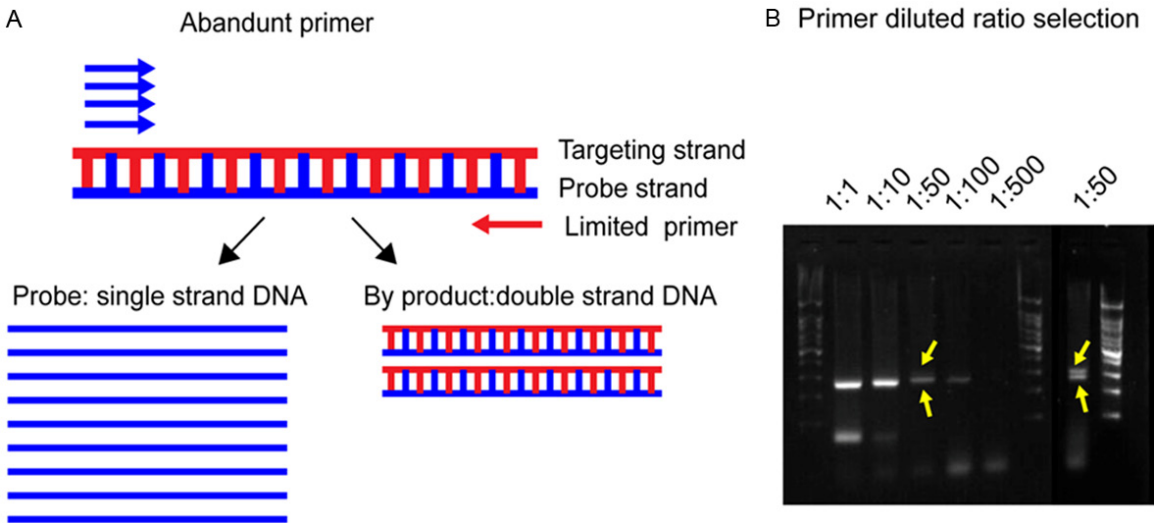

Figure S1. The principle of asymmetric PCR-derived single-standed DNA probes in flurescent in situ hybridization for lncRNA localization in mitochondria. A: The principle of asymmetric PCR for making probes. B: PCR results of primer dilution ratio.